Catalysis Science & Technology

PAPER

View Article Online
View Journal | View Issue

Cite this: *Catal. Sci. Technol.*, 2015, 5, 3728

Tuning the chemoselective hydrogenation of aromatic ketones, aromatic aldehydes and quinolines catalyzed by phosphine functionalized ionic liquid stabilized ruthenium nanoparticles†

He-yan Jiang* and Xu-xu Zheng

Received 28th February 2015,
Accepted 15th May 2015

DOI: 10.1039/c5cy00293a

www.rsc.org/catalysis

Ruthenium nanoparticles (Ru NPs) stabilized by phosphine-functionalized ionic liquids (PFILs) were synthesized in an imidazolium-based ionic liquid using H_2 as a reductant. Characterization showed well-dispersed particles of about 2.2 nm (TEM) and confirmed the PFIL stabilization of the Ru NPs (NMR). The Ru NPs stabilized by PFILs exhibited excellent activity and switchable chemoselectivity in the heterogeneous selective hydrogenation of aromatic ketones, aromatic aldehydes and quinolines under mild conditions.

Introduction

Metal nanoparticles are fascinating because of their applications in areas such as optoelectronics, sensing, medicine and catalysis.[1–5] The investigation of metal nanoparticles in catalysis has been receiving increasing interest because nanometal particles present an efficient combination of the advantages of heterogeneous and homogeneous catalysts. Additional stabilization, generally provided by phosphines, amines or polymers, of nanoparticles influences the catalytic activity, selectivity and recyclability.[6–12] Ionic liquid-stabilized metal nanoparticles are interesting new catalytic materials for hydrogenation and other applications.[3] Furthermore, with both covalent and electrostatic stabilization, functionalized ionic liquids containing metal-binding moieties have been gradually employed in the synthesis of transition metal nanoparticles to improve the catalytic system stability and/or catalytic performance.[13–17] However, up to now, ionic liquid-stabilized metal nanoparticles have been tested as catalysts mainly in the hydrogenation of alkenes or arenes.[3,18–21]

The chemoselective reduction of aromatic compounds (aromatic ketones, aromatic aldehydes, quinolines, *etc.*) by means of heterogeneous catalysis is an important field in the industrial hydrogenation process.[22–31] Furthermore, tuning the hydrogenation chemoselectivity of aromatic compounds in heterogeneous catalysis remains a formidable scientific challenge. We focus on the selective hydrogenation of aromatic compounds, an important organic transformation, since the resulting products are versatile precursors to many natural products and drug molecules. As part of our ongoing research,[32–34] we herein disclose a practical, general, and efficient method by which aromatic compounds can be hydrogenated with switchable excellent chemoselectivity under mild conditions catalyzed by ruthenium nanoparticles (Ru NPs) stabilized by phosphine-functionalized ionic liquids (PFILs). To the best of our knowledge, the approach used here has not been explored before.

Results and discussion

Synthesis and characterization of ruthenium nanoparticles

The synthesis of Ru NPs was achieved through the reduction of $RuO_2{\cdot}xH_2O$ or Ru(COD)(2-methylallyl)$_2$ (COD = cycloocta-1,5-diene)

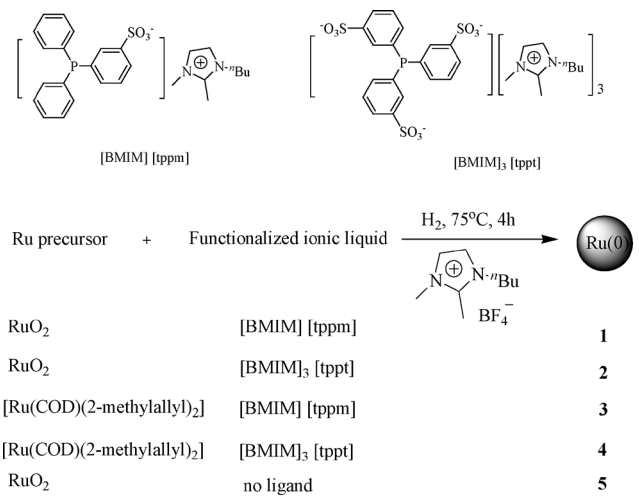

Fig. 1 Synthesis of Ru NPs in [BMIM]BF_4.

Key Laboratory of Catalysis Science and Technology of Chongqing Education Commission, Chongqing Key Laboratory of Catalysis and Functional Organic Molecules, Chongqing Technology and Business University, Chongqing 400067, PR China. E-mail: orgjiang@163.com; Fax: +86 23 6276 9652; Tel: +86 23 6276 9652

† Electronic supplementary information (ESI) available. See DOI: 10.1039/c5cy00293a

in [BMIM]BF_4 (BMIM = 1-butyl-2,3-dimethylimidazolium) under H_2 atmosphere (1 MPa) in the presence of 1.0 equivalent of PFILs [BMIM][tppm] or [BMIM][tppt] (Fig. 1), which afforded a dark suspension. For comparison, Ru NPs were also synthesized in [BMIM]BF_4 in the absence of any additional stabilizer. A black powder could be isolated from the black suspension by adding acetone and then centrifuging (8000 rpm for 10 min). After being washed three times with acetone and dried under reduced pressure, the isolated powder was analyzed by transmission electron microscopy (TEM), X-ray photoelectron spectroscopy (XPS), X-ray diffraction (XRD), nuclear magnetic resonance (NMR) and infrared spectroscopy (IR).

TEM analysis was conducted to characterize the isolated Ru NPs and determine their mean diameter (Fig. 2). In general, Ru NPs prepared from the precursor $RuO_2{\cdot}xH_2O$ showed better dispersion than those from [Ru(COD)(2-methylallyl)$_2$] (Fig. 2, images 1 and 2 *versus* 3 and 4), and the TEM image showed a trend toward agglomeration of the Ru NPs in the absence of a functionalized ionic liquid (Fig. 2, image 5). The TEM image of isolated Ru NPs **1**, derived from $RuO_2{\cdot}xH_2O$, showed the formation of nearly monodispersed Ru nanoparticles with an average diameter of 2.2 nm.

XPS analysis of the isolated Ru NPs **1** was carried out to elucidate the nature of the stabilizing layer of the nanometal particles. XPS analysis of Ru NPs stabilized by [BMIM][tppm] showed the presence of ruthenium, phosphorus, nitrogen and carbon, which signified the presence of [BMIM][tppm] in the ligand sphere of the Ru NPs. The X-ray diffraction pattern of the isolated Ru NPs **1** (Fig. 3) generally showed the predicted lines of the Ru hcp structure in the wide-angle range.

^{31}P NMR studies of [BMIM][tppm] and [BMIM][tppm] stabilized Ru NPs **1** in [BMIM]BF_4 were conducted. The ^{31}P NMR spectrum of [BMIM][tppm] showed a peak at δ = −5.4 ppm. However, no signal was detected in the ^{31}P NMR spectrum of Ru NPs **1**. After the mixture of isolated Ru NPs **1** and hydrogen peroxide was further stirred at 50 °C for 10 h, an oxide signal of [BMIM][tppm] appeared at δ = 30.0 ppm. The ^{31}P NMR observations may be explained by the fact that majority of the [BMIM][tppm] were attached to the Ru NP surface, and free phosphine and attached phosphine exchange very fast, affording no ^{31}P NMR signal.

IR is effective for the investigation of the mutual ligand–metal interactions of nanometal catalysts. Information on the interaction between the nanometal and the phosphine in Ru NPs **1** was confirmed by FTIR methods in which the red shift of the P–C_6H_5 deformation around 1469 cm^{-1} in Ru NPs **1** is an indication of the coordination of [BMIM][tppm] to the metal Ru(0).

The effect of [BMIM][tppm] in the catalyst is noteworthy. Due to the strong coordination capacity of the anion of [BMIM][tppm], Ru NPs were well dispersed and highly stable in catalytic hydrogenation. On the basis of these results, it was deduced that the [$P(C_6H_5)_2(C_6H_4$-*m*-$SO_3)^-$] ions formed a layer around the surface of the Ru NPs, leading to a sphere of negative charge, and then the cation of [BMIM][tppm] was arranged into an outer layer for charge conservation (Fig. 4). Recently, several groups have demonstrated that ionic liquids possess self-organized structures, which can create an external layer around the surface of the metal NPs to protect them from aggregation.[5,20,35]

Catalytic hydrogenation

Initially, we chose styrene as a model substrate to explore the catalytic performance of Ru NPs **1** under very mild conditions (30 °C, H_2 at 1 MPa). Fig. 5 shows the effect of the conversion

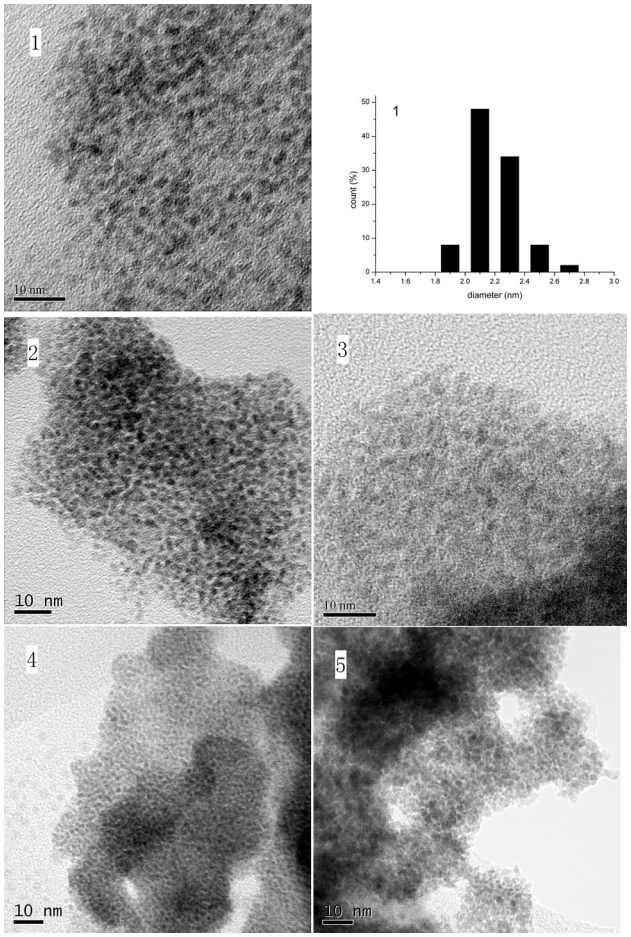

Fig. 2 TEM images of Ru nanoparticles **1**, **2**, **3**, **4** and **5**.

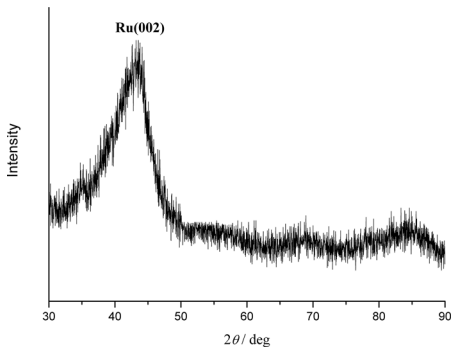

Fig. 3 X-Ray diffraction pattern of isolated Ru NPs **1**.

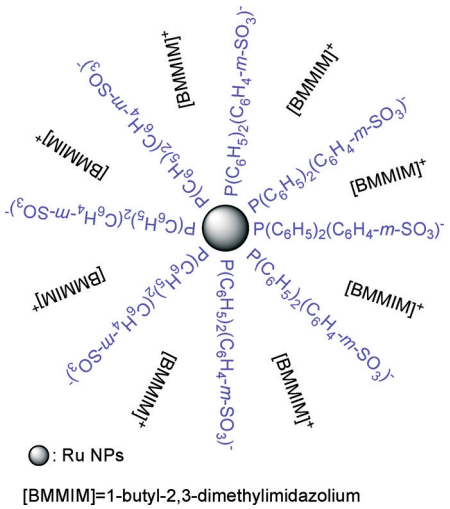

Fig. 4 The PFIL ([BMIM][tppm]) stabilized/modified Ru nanoparticles.

versus time. The hydrogenation of styrene produced only ethylbenzene in the test. It was found that the conversion increased linearly with time, showing no induction period, proving that this catalyst did not convert into other catalytically active species. Furthermore, mercury-poisoning experiments were run as they can selectively poison metal nanoparticles, by forming an amalgam with mercury, to help distinguish between homogeneous and heterogeneous catalysts.[36] In such an experiment, the conversion was 61.6% after the initial 1 hour; mercury was then added under argon atmosphere and the reaction was completely terminated as evidenced by the absence of change in the conversion after an additional reaction time of 3 hours. In addition, it was found that the amount of leaching from Ru NPs **1** was about 0.9 ppm by ICP-AES analysis of the organic phase in styrene catalytic hydrogenation. The catalyst could be reused by simple liquid–liquid extraction after the reaction. The procedure was repeated ten times and the results indicated that Ru NPs **1** could be recycled without any loss of catalytic activity (Fig. 6). The average diameter of the spent Ru NPs **1** after ten

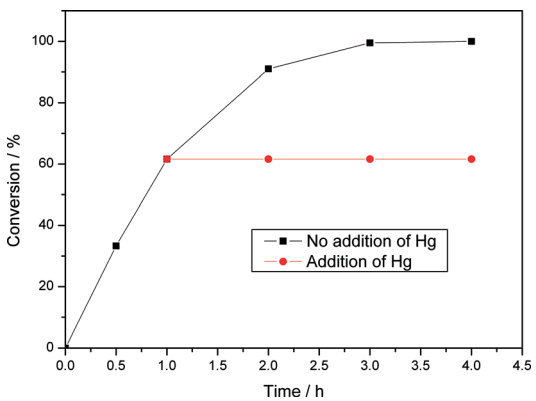

Fig. 5 Reaction profiles for hydrogenation of styrene and Hg^0 poisoning of Ru NPs **1**. Reaction conditions: styrene (8.9×10^{-3} mol; styrene/Ru = 500), 30 °C, H_2 at 1 MPa.

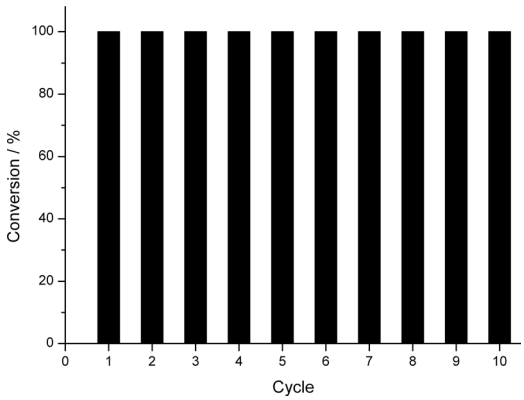

Fig. 6 Recyclability of Ru NPs **1** for the hydrogenation of styrene. Reaction conditions: styrene (8.9×10^{-3} mol; styrene/Ru = 500), 30 °C, H_2 at 1 MPa.

recycles of styrene hydrogenation was 2.13 nm (S2 and S3 in the ESI†). All the results above strongly supported the proposal that the reaction progressed under heterogeneous catalysis rather than homogeneous catalysis.

The chemoselective reduction of carbonyl compounds by means of heterogeneous catalysis is of considerable importance in the synthesis of fine chemicals, particularly intermediates in the fragrance and pharmaceutical industries.[22–25] Baiker and coworkers found that Pd-[BMIm][PF_6] exhibited good activity and selectivity in the hydrogenation of acetophenone.[23] However, tuning the hydrogenation chemoselectivity of aromatic carbonyl compounds in heterogeneous catalysis remains rather difficult. The effect of different reaction factors on the chemoselective hydrogenation of acetophenone is listed in Table 1. The importance of a basic additive in a catalyst system for the selective hydrogenation of aromatic ketones has been well-established.[37,38] The Ru NPs had no catalytic activity at ambient temperature in [BMIM]BF_4 in the absence of a basic additive (Table 1, entry 1). Similar to previous reports, a basic additive was helpful to improve the catalytic performance; acetophenone could be hydrogenated with 77.0% conversion and 99.0% chemoselectivity to 1-phenylethanol in the presence of [BMIM]OH (1-butyl-2,3-dimethylimidazolium hydroxide) (Table 1, entry 2). The PFIL stabilizers showed an important influence on the catalytic process; without the stabilizer, the hydrogenation resulted in a conversion of 94% and a chemoselectivity as low as 76.6% to 1-phenylethanol (Table 1, entry 4). Ru NPs stabilized by [BMIM][tppm] showed lower activity but higher chemoselectivity to 1-phenylethanol than Ru NPs stabilized by [BMIM][tppt] (Table 1, entries 2–3). These results indicated that PFILs not only stabilized the metal particles in the preparation of the catalyst, but also served to additionally modify the Ru NPs in the chemoselective hydrogenation.

Since the properties of the metal precursors greatly influence the particle size and dispersion of nanometal catalysts,[3,4] metal precursors, including $RuO_2 \cdot xH_2O$ and [Ru(COD)(2-methylallyl)$_2$], were tested. Generally, Ru NPs **1** and **2**, prepared from $RuO_2 \cdot xH_2O$, showed higher activity

Table 1 Optimization of reaction conditions for the chemoselective hydrogenation of acetophenone by Ru NPs[a]

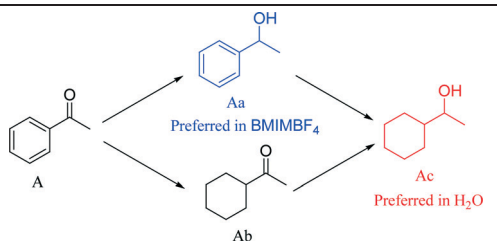

Entry	Catalyst	Solvent	t (h)	Conversion (%)	Selectivity (%) Aa	Ab	Ac
1	**1**	$BMIMBF_4$	15	0.0	—	—	—
2	**1**[b]	$BMIMBF_4$	15	77.0	99.0	0.4	0.6
3	**2**[b]	$BMIMBF_4$	15	92.0	84.0	6.2	9.8
4	**5**[b]	$BMIMBF_4$	15	94.0	76.6	3.4	20.0
5	**3**[b]	$BMIMBF_4$	15	48.0	94.2	2.9	2.9
6	**4**[b]	$BMIMBF_4$	15	69.0	92.6	2.7	4.7
7	Ru/C[b]	$BMIMBF_4$	15	0.0	—	—	—
8	**1**[c]	H_2O	1	100.0	0.0	0.4	99.6
9	**5**[c]	H_2O	1	26.1	55.9	18.4	25.7
10	Ru/C	H_2O	1	99.0	34.6	1.2	64.2

[a] Reaction was carried out at 30 °C. Substrate: in a 1 ml solution at 1.8 M, P_{H_2}: 5.0 MPa. Substrate/Ru = 100 : 1, Ru/C (5 wt%, 36 mg). Products were analyzed by using a GC instrument with an FID detector and a β-DEX120 capillary column. [b] [BMIM]OH = 0.20 mol L^{-1} was added. [c] Ru nanoparticles were isolated and redispersed in water.

Table 2 Chemoselective hydrogenation of aromatic ketones catalyzed by Ru NPs **1**[a]

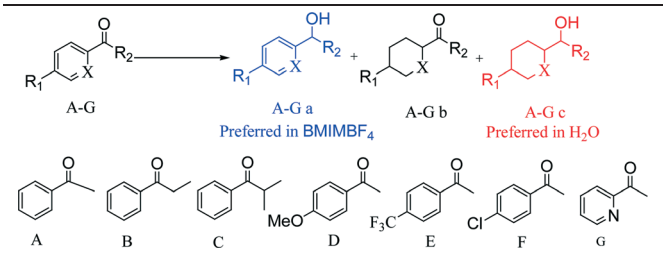

Entry	A–G	Solvent	t (h)	Conversion (%)	Selectivity (%) A–G a	A–G b	A–G c
1	A	$BMIMBF_4$	15	77.0	99.0	0.4	0.6
2[b]	A	H_2O	1	100.0	0.0	0.4	99.6
3	B	$BMIMBF_4$	15	21.0	86.0	14.0	0.0
4[b]	B	H_2O	2	100.0	0.0	4.5	95.5
5	C	$BMIMBF_4$	15	10.4	80.0	20.0	0.0
6[b]	C	H_2O	2	72.5	21.0	38.0	41.0
7	D	$BMIMBF_4$	15	2.0	100.0	0.0	0.0
8[b]	D	H_2O	2	99.0	0.0	0.0	100.0
9	E	$BMIMBF_4$	15	100.0	100.0	0.0	0.0
10[b]	E	H_2O	2	100.0	92.1	3.3	4.6
11	F	$BMIMBF_4$	15	72.0	85.0	9.7	5.3
12[b]	F	H_2O	2	59.3	93.3	0.3	6.4
13	G	$BMIMBF_4$	15	26.4	96.7	0.0	3.3
14[b]	G	H_2O	2	100.0	0.0	0.0	100.0

[a] The reaction conditions are the same as in Table 1. When $BMIMBF_4$ was the solvent, [BMIM]OH = 0.20 mol L^{-1} was added. [b] Ru nanoparticles **1** were isolated and redispersed in water.

than **3** and **4**, which were prepared from [Ru(COD)(2-methylallyl)$_2$] (Table 1, entries 2–3 *versus* 5–6). The best chemoselectivity of 99.0% was achieved in the hydrogenation of acetophenone to 1-phenylethanol using Ru NPs **1** as the catalyst.

The best condition is when there is no solvent, and if a solvent is needed then water is preferred.[39] Indeed, water is an attractive alternative to traditional organic solvents because it is cheap, readily available, nontoxic, non-flammable and safe to the environment. Ru NPs **1** isolated from centrifugation were redispersed in water to test the catalytic performance (Table 1, entry 8). To our surprise, when water was used as the solvent in the hydrogenation of acetophenone, the reaction progressed very fast with a high chemoselectivity to cyclohexylethanol. In comparison with the catalytic hydrogenation in the ionic liquid $BMIMBF_4$, the high catalytic activity in water may be attributed to the increased substrate solubility in water as well as the interactions between water and the substrate *via* hydrogen bonding.[40] However, Ru NPs **5** isolated from centrifugation and redispersed in water showed poor activity and chemoselectivity (Table 1, entry 9).

A commercially available Ru/C catalyst was also tested under similar reaction conditions in the hydrogenation of acetophenone (Table 1, entries 7 and 10). Overall, the Ru/C catalyst showed poor activity and chemoselectivity towards either 1-phenylethanol or cyclohexylethanol.

Some representative examples are listed in Table 2 for the chemoselective hydrogenation of aromatic ketones catalyzed by Ru NPs **1** in both [BMIM]BF_4 and water. The extent of the chemoselectivity appears to be delicately influenced by the substituent in the substrate. In general, the activity and chemoselectivity decreased by increasing the bulkiness of the alkyl group from methyl or primary alkyl to isopropyl (Table 2, entries 1–6). It was found that when the substituent is in the *para* position, the substrate with an electron-donating group showed poor reaction activity with excellent chemoselectivity to the C=O hydrogenation product in [BMIM]BF_4 or the full hydrogenation product in water (Table 2, entries 7–8), and substrates with electron-withdrawing groups showed good reaction activity with the major chemoselectivity to C=O hydrogenation products in both [BMIM]BF_4 and water (Table 2, entries 9–12). Furthermore, 2-acetothiophene, 2-acetopyridine, and 2-acetopyrrole were also tested; 2-acetothiophene and 2-acetopyrrole showed no reaction activity during the test. The chemoselectivity of 2-acetopyridine to C=O and full hydrogenation products could reach 96.7% and 100%, respectively (Table 2, entries 13–14). The effect of the steric bulk and the electronic nature of the substrates influence the activity and chemoselectivity of the reaction.

The chemoselective hydrogenation of aromatic aldehydes was also tested (Table 3). In comparison with the chemoselective hydrogenation of aromatic ketones, aromatic aldehydes could be hydrogenated to the corresponding C=O and full hydrogenation products easily. Without the basic additive, benzaldehyde could be hydrogenated to the corresponding benzyl alcohol in [BMIM]BF_4 (Table 3, entry 1). The complete

Table 3 Chemoselective hydrogenation of aromatic aldehydes catalyzed by Ru NPs **1**[a]

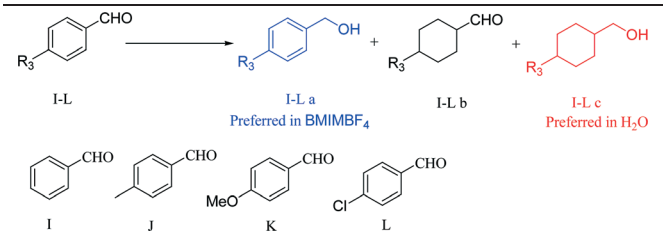

Entry	I–L	Solvent	t (h)	Conversion (%)	Selectivity (%) I–L a	I–L b	I–L c
1	I	$BMIMBF_4$	15	100.0	100.0	0.0	0.0
2[b]	I	H_2O	1	100.0	0.0	0.0	100.0
3	J	$BMIMBF_4$	15	30.5	100.0	0.0	0.0
4[b]	J	H_2O	1	94.7	96.6	0.0	3.4
5[b]	J	H_2O	3	100.0	0.5	0.0	99.5
6	K	$BMIMBF_4$	15	0.0	—	—	—
7[b]	K	H_2O	1	99.8	97.0	0.0	3.0
8[b]	K	H_2O	3	100.0	87.9	0.0	12.1
9	L	$BMIMBF_4$	15	97.2	100.0	0.0	0.0
10[b]	L	H_2O	1	97.8	0.1	0.0	99.9
11[b]	L	H_2O	3	100.0	0.0	0.0	100.0

[a] Reaction was carried out at 30 °C. Substrate: in a 1 ml solution at 1.8 M, P_{H_2}: 3.0 MPa. Substrate/Ru = 100 : 1. Products were analyzed by using a GC instrument with an FID detector and a β-DEX120 capillary column. [b] Ru nanoparticles **1** were isolated and redispersed in water.

hydrogenation product of benzaldehyde could be achieved in water (Table 3, entry 2). When the substituent is in the *para* position of benzaldehyde, C═O and full hydrogenation could be achieved in weak electron-donating group and electron-withdrawing group substituted substrates (Table 3, entries 3–5 and 9–11). With a strong electron-donating group in the *para* position, *p*-anisaldehyde could be hydrogenated with the major chemoselectivity to the C═O hydrogenation product during our test (Table 3, entries 6–8).

Hydrogenation of quinoline and its derivatives is of considerable industrial interest for the production of petrochemicals, fine chemicals, and pharmaceuticals.[26–28] However, tuning the hydrogenation chemoselectivity of quinolines in heterogeneous catalysis under mild conditions remains a formidable scientific challenge. We investigated the catalytic performance of Ru NPs for the hydrogenation of quinoline and its derivatives (Table 4). Quinoline could be easily hydrogenated to 1,2,3,4-tetrahydroquinoline at 50 °C with 98.0% chemoselectivity in $[BMIM]BF_4$ and 99.0% chemoselectivity in water (Table 4, entries 1–2). Unprecedentedly, complete hydrogenation of quinoline could also be achieved with 98.2% chemoselectivity in water at a reaction temperature as low as 60 °C (Table 4, entry 3). A commercially available Ru/C catalyst was also tested under similar reaction conditions in the hydrogenation of quinoline (Table 4, entries 4–6). The Ru/C catalyst showed poor activity with the major chemoselectivity to 1,2,3,4-tetrahydroquinoline during the test. Quinoline analogues were also tested. Generally, the hydrogenation activity of 2- or 3-methylquinoline was almost the same as quinoline. The presence of a substituent in the

Table 4 Chemoselective hydrogenation of quinoline and derivatives catalyzed by Ru NPs **1**[a]

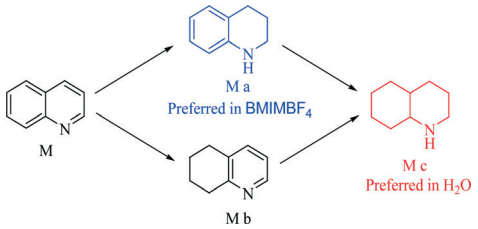

Entry	Catalyst	M–P	Solvent	T (°C)	Conversion (%)	Selectivity (%) M–P a	M–P b	M–P c
1	**1**	M	$BMIMBF_4$	50	95.0	98.0	2.0	0.0
2	**1**[b,c]	M	H_2O	50	93.0	99.0	0.3	0.7
3	**1**[c]	M	H_2O	60	98.6	1.8	0.0	98.2
4	Ru/C	M	$BMIMBF_4$	50	67.0	98.0	2.0	0.0
5	Ru/C[b]	M	H_2O	50	30.0	98.6	0.0	1.4
6	Ru/C	M	H_2O	60	92.0	75.9	22.5	1.6
7	**1**	N	$BMIMBF_4$	50	98.4	96.0	4.0	0.0
8	**1**[b,c]	N	H_2O	50	81.3	55.5	44.5	0.0
9	**1**[c]	N	H_2O	60	97.7	1.3	30.4	68.3
10	**1**	O	$BMIMBF_4$	50	97.9	87.7	0.0	12.3
11	**1**[b,c]	O	H_2O	50	86.8	24.4	0.0	75.6
12	**1**[c]	O	H_2O	60	100.0	0.0	0.0	100.0
13	**1**	P	$BMIMBF_4$	50	46.0	100.0	0.0	0.0
14	**1**[b,c]	P	H_2O	50	71.7	100.0	0.0	0.0
15	**1**[c]	P	H_2O	60	95.8	100.0	0.0	0.0

[a] Reaction conditions: substrate in a 1 ml solution at 1.8 M, P_{H_2}: 5.0 MPa. Substrate/Ru = 100 : 1, Ru/C (5 wt%, 36 mg). Products were analyzed by using a GC instrument with an FID detector and an HP-5 column, reaction time: 15 h. [b] Reaction time: 1 h. [c] Ru nanoparticles **1** were isolated and redispersed in water.

2-position of quinoline would cause the decrease of the hydrogenation chemoselectivity due to the steric hindrance. Introducing a methyl group in the quinoline molecule, especially in the 3-position of quinoline, obviously promoted the formation of decahydroquinoline (Table 4, entry 12). 8-Methylquinoline could be hydrogenated with absolute chemoselectivity to 1,2,3,4-tetrahydroquinoline during the test (Table 4, entries 13–15).

Conclusions

The results of this study demonstrated that PFIL-stabilized Ru NPs are effective catalysts for the challenging selective hydrogenation of aromatic ketones, aromatic aldehydes and quinolines with a distinct high and switchable selectivity towards different functional groups of substrates. The catalytic performance is complementary to both classical homogeneous and heterogeneous catalysis. Additional work is currently in progress in this and related areas.

Experimental section

Materials

All manipulations involving air-sensitive materials were carried out using standard Schlenk line techniques under an

atmosphere of nitrogen. $RuO_2{\cdot}xH_2O$, Ru(COD)(2-methylallyl)$_2$ and Ru/C (5%) were purchased from Acros. Various substrates and other reagents were of analytical grade. The purity of hydrogen was over 99.99%. Phosphine-functionalized ionic liquids were synthesized according to the literature.[41,42] Products were analyzed by using a GC instrument (cyclohexylcyclohexane used as an internal standard) with an FID detector and an HP-5 column (30 m × 0.25 mm)/β-DEX120 capillary column (25 m × 0.25 mm). Products were confirmed by GC-MS and NMR. TEM analyses were performed using a JEOL JEM 2010 transmission electron microscope operating at 200 kV with a nominal resolution of 0.25 nm. X-ray photoelectron spectroscopy (XPS) measurements were performed on a Thermo ESCALAB 250 spectrometer. XRD analysis was performed with a D/MAX 2550 VB/PC using a graphite crystal as a monochromator. Ru and P contents were characterized using a Perkin Elmer Optima 2100DV ICP-AES (S1 in the ESI†).

Synthesis of ruthenium nanoparticles

Preparation of nanocatalysts 1, 2 or 5. In a typical experiment, $RuO_2{\cdot}xH_2O$ (0.018 mmol) and PFILs (0.018 mmol for **1** and **2**, no ligand for **5**) were dispersed in [BMIM]BF_4 (1 mL) (BMIM = 1-butyl-2,3-dimethylimidazolium) and the reaction mixture was placed in a 20 mL stainless-steel high pressure reactor. After stirring the mixture at room temperature under an atmosphere of N_2 for 30 min, a constant pressure of H_2 (1 MPa) was introduced to the system and the content was stirred for 4 h at 75 °C. The reactor was cooled to ambient temperature and carefully vented. A dark solution was obtained. The Ru NPs embedded in [BMIM]BF_4 were employed for hydrogenation studies (see below). Isolation of the Ru NPs for TEM, XPS, XRD analysis and for catalytic experiments (see below) was achieved by dissolving the mixture in acetone (5 mL), centrifuging (8000 rpm for 10 min), washing with acetone (2 × 5 mL) and drying under vacuum. Furthermore, the supernatant of the [BMIM][tppm]-stabilized Ru NPs **1** was analyzed by ICP-AES methods and about 2.2% Ru and 5.4% [BMIM][tppm] were lost during the washing and drying procedure.

Preparation of nanocatalysts 3 or 4. In a typical experiment, Ru(COD)(2-methylallyl)$_2$ (0.018 mmol) and PFILs (0.018 mmol) were dispersed in [BMIM]BF_4 (1 mL) and the reaction mixture was placed in a 20 mL stainless-steel high pressure reactor. After stirring the mixture at room temperature under an atmosphere of N_2 for 30 min, a constant pressure of H_2 (1 MPa) was introduced to the system and the content was stirred for 4 h at 75 °C. The reactor was cooled to ambient temperature and carefully vented. A dark brown solution was obtained which was used for the hydrogenation reaction (see below). Isolation of the Ru NPs for TEM analysis and catalytic experiments (see below) was achieved by dissolving the mixture in acetone (5 mL), centrifuging (8000 rpm for 10 min), washing with acetone (2 × 5 mL) and drying under vacuum.

General procedure for the heterogeneous chemoselective hydrogenation

In [BMIM]BF_4. The stainless steel autoclave containing the previously prepared PFIL-stabilized Ru(0) catalyst was charged with the appropriate substrate, then the autoclave was sealed and purged with pure hydrogen several times. After the reactants were heated to predetermined temperature, the reaction timing began. After completion of the reaction and cooling to ambient temperature, the products were isolated by liquid–liquid extraction with diethyl ether and analyzed by gas chromatography.

In water. The isolated nanoparticles dispersed in water (1 ml) were placed in a stainless steel autoclave, and the substrate was added. Then the autoclave was sealed and purged with pure hydrogen several times. After the reactants were heated to predetermined temperature, the reaction timing began. After completion of the reaction and cooling to ambient temperature, the products were isolated by liquid–liquid extraction with diethyl ether or centrifugation and analyzed by gas chromatography.

Acknowledgements

This work was financially supported by the National Natural Science Foundation of China (no. 21201184), Natural Science Foundation Project of CQ (no. cstc2014jcyjA10105), Ministry of Education of Chongqing (no. KJ1400601), Chongqing Key Laboratory of Catalysis and Functional Organic Molecules (no. 1456028) and 100 Leading Scientists Promotion Project of Chongqing.

Notes and references

1 K. J. Klabunde and R. M. Richards, *Nanoscale Materials in Chemistry*, Wiley-Interscience, New York, 2001.
2 G. Schmid, *Clusters and Colloids. From Theory to Applications*, Wiley VCH, Weinheim, 2004.
3 J. Dupont and J. D. Scholten, *Chem. Soc. Rev.*, 2010, **39**, 1780–1804.
4 Y. Yuan, N. Yan and P. J. Dyson, *ACS Catal.*, 2012, **2**, 1057–1069.
5 K. L. Luska and A. Moores, *ChemCatChem*, 2012, **4**, 1534–1546.
6 Y. M. A. Yamada, T. Arakawa, H. Hocke and Y. Uozumi, *Angew. Chem., Int. Ed.*, 2007, **46**, 704–706.
7 D. Astruc, F. Lu and J. R. Aranzaes, *Angew. Chem., Int. Ed.*, 2005, **44**, 7852–7872.
8 S. Jansat, M. Gomez, K. Philippot, G. Muller, E. Guiu, C. Claver, S. Castillon and B. Chaudret, *J. Am. Chem. Soc.*, 2004, **126**, 1592–1593.
9 H. Mao, J. Ma, Y. Liao, S. Zhao and X. Liao, *Catal. Sci. Technol.*, 2013, **3**, 1612–1617.
10 G. S. Fonseca, A. P. Umpierre, P. F. P. Fichtner, S. R. Teixeira and J. Dupont, *Chem. – Eur. J.*, 2003, **9**, 3263–3269.
11 C. Vollmer, E. Redel, K. Abu-Shandi, R. Thomann, H. Manyar, C. Hardacre and C. Janiak, *Chem. – Eur. J.*, 2010, **16**, 3849–3858.

12 P. S. Roy and S. K. Bhattacharya, *Catal. Sci. Technol.*, 2013, **3**, 1314–1323.
13 R. R. Dykeman, N. Yan, R. Scopelliti and P. J. Dyson, *Inorg. Chem.*, 2011, **50**, 717–719.
14 H. Zhang and H. Cui, *Langmuir*, 2009, **25**, 2604–2612.
15 D. B. Zhao, Z. F. Fei, T. J. Geldbach, R. Scopelliti and P. J. Dyson, *J. Am. Chem. Soc.*, 2004, **126**, 15876–15882.
16 N. Kocharova, J. Leiro, J. Lukkari, M. Heinonen, T. Skala, F. Sutara, M. Skoda and M. Vondracek, *Langmuir*, 2008, **24**, 3235–3242.
17 B. Zhang, Y. Yuan, K. Philippot and N. Yan, *Catal. Sci. Technol.*, 2015, **5**, 1683–1692.
18 J. Dupont, G. S. Fonseca, A. P. Umpierre, P. F. P. Fichtner and S. R. Teixeira, *J. Am. Chem. Soc.*, 2002, **124**, 4228–4229.
19 A. Denicourt-Nowicki, B. Leger and A. Roucoux, *Phys. Chem. Chem. Phys.*, 2011, **13**, 13510–13517.
20 W. Zhu, Y. Yu, H. Yang, L. Hua, Y. Qiao, X. Zhao and Z. Hou, *Chem. – Eur. J.*, 2013, **19**, 2059–2066.
21 E. Redel, J. Kramer, R. Thomann and C. Janiak, *J. Organomet. Chem.*, 2009, **694**, 1069–1075.
22 E. T. Silveira, A. P. Umpierre, L. M. Rossi, G. Machado, J. Morais, G. V. Soares, I. J. R. Baumvol, S. R. Teixeira, P. F. P. Fichtner and J. Dupont, *Chem. – Eur. J.*, 2004, **10**, 3734–3740.
23 F. Jutz, J. M. Andanson and A. Baiker, *J. Catal.*, 2009, **268**, 356–366.
24 J. Julis, M. Hölscher and W. Leitner, *Green Chem.*, 2010, **12**, 1634–1639.
25 D. Gonzalez-Galvez, P. Lara, O. Rivada-Wheelaghan, S. Conejero, B. Chaudret, K. Philippot and P. W. N. M. van Leeuwen, *Catal. Sci. Technol.*, 2013, **3**, 99–105.
26 D. Zhu, H. Jiang, L. Zhang, X. Zheng, H. Fu, M. Yuan, H. Chen and R. Li, *ChemCatChem*, 2014, **6**, 2954–2960.
27 L. Zhang, X. Wang, Y. Xue, X. Zeng, H. Chen, R. Li and S. Wang, *Catal. Sci. Technol.*, 2014, **4**, 1939–1948.
28 Y. Sun, H. Fu, D. Zhang, R. Li, H. Chen and X. Li, *Catal. Commun.*, 2010, **12**, 188–192.
29 G. S. Fonseca, J. D. Scholten and J. Dupont, *Synlett*, 2004, 1525–1528.
30 V. Kogan, Z. Aizenshtat and R. Neumann, *New J. Chem.*, 2002, **26**, 272–274.
31 C. Chen, H. Chen and W. Cheng, *Appl. Catal., A*, 2003, **248**, 117–128.
32 H. Y. Jiang, C. F. Yang, C. Li, H. Y. Fu, H. Chen, R. X. Li and X. J. Li, *Angew. Chem., Int. Ed.*, 2008, **47**, 9240–9244.
33 H. Y. Jiang, B. Sun, X. X. Zheng and H. Chen, *Appl. Catal., A*, 2012, **421–422**, 86–90.
34 H. Y. Jiang and X. X. Zheng, *Appl. Catal., A*, 2015, **499**, 118–123.
35 Z. F. Wu and H. Y. Jiang, *RSC Adv.*, 2015, **5**, 34622–34629.
36 R. A. Sheldon, M. Wallau, I. W. C. E. Arends and U. Schuchardt, *Acc. Chem. Res.*, 1998, **31**, 485–493.
37 T. Ohkuma, H. Ooka, T. Ikariya and R. Noyori, *J. Am. Chem. Soc.*, 1995, **117**, 2675–2676.
38 A. Perosa, P. Tundo and M. Selva, *J. Mol. Catal. A: Chem.*, 2002, **180**, 169–175.
39 R. A. Sheldon, *Green Chem.*, 2005, **7**, 267–278.
40 L. Foppa and J. Dupont, *Chem. Soc. Rev.*, 2015, **44**, 1886–1897.
41 C. P. Mehnert, R. A. Cook, N. C. Dispenziere and E. J. Mozeleski, *Polyhedron*, 2004, **23**, 2679–2688.
42 S. Wesselbaum, U. Hintermair and W. Leitner, *Angew. Chem., Int. Ed.*, 2012, **51**, 8585–8588.

